Theoretical investigation of fabrication-related disorders on the properties of subwavelength metal-dielectric-metal plasmonic waveguides

Changjun Min[1] and Georgios Veronis[1,2*]

[1]*Center for Computation and Technology, Louisiana State University, Baton Rouge, Louisiana 70803 USA*
[2]*Department of Electrical and Computer Engineering, Louisiana State University, Baton Rouge, Louisiana 70803USA*
**gveronis@lsu.edu*

Abstract: We theoretically investigate the effect of fabrication-related disorders on subwavelength metal-dielectric-metal plasmonic waveguides. We use a Monte Carlo method to calculate the roughness-induced excess attenuation coefficient with respect to a smooth waveguide. For small roughness height, the excess optical power loss due to disorder is small compared to the material loss in a smooth waveguide. However, for large roughness height, the excess attenuation increases rapidly with height and the propagation length of the optical mode is severely affected. We find that the excess attenuation is mainly due to reflection from the rough surfaces. However, for small roughness correlation lengths, enhanced absorption is the dominant loss mechanism due to disorder. We also find that the disorder attenuation due to reflection is approximately maximized when the power spectral density of the disordered surfaces at the Bragg spatial frequency is maximized. Finally, we show that increasing the modal confinement or decreasing the guide wavelength, increase the attenuation due to disorder.

OCIS codes: (240.6680) Surface Plasmons; (130.2790) Guided waves; (240.5770) Roughness.

References and links

1. W. L. Barnes, A. Dereux, and T. W. Ebbesen, "Surface plasmon subwavelength optics," Nature **424**(6950), 824–830 (2003).
2. E. Ozbay, "Plasmonics: merging photonics and electronics at nanoscale dimensions," Science **311**(5758), 189–193 (2006).
3. R. Zia, J. A. Schuller, A. Chandran, and M. L. Brongersma, "Plasmonics: the next chip-scale technology," Mater. Today **9**(7–8), 20–27 (2006).
4. S. A. Maier, *Plasmonics: fundamentals and applications*, (Springer, New York, 2007).
5. H. A. Atwater, "The promise of plasmonics," Sci. Am. **296**(4), 56–62 (2007).
6. R. Zia, M. D. Selker, P. B. Catrysse, and M. L. Brongersma, "Geometries and materials for subwavelength surface plasmon modes," J. Opt. Soc. Am. A **21**(12), 2442–2446 (2004).
7. G. Veronis, and S. Fan, "Bends and splitters in subwavelength metal-dielectric-metal plasmonic waveguides," Appl. Phys. Lett. **87**(13), 131102 (2005).
8. S. E. Kocabas, G. Veronis, D. A. B. Miller, and S. Fan, "Modal analysis and coupling in metal-insulator-metal waveguides," Phys. Rev. B **79**(3), 035120 (2009).
9. D. M. Pozar, *Microwave Engineering*, (Wiley, New York, 1998).
10. E. N. Economou, "Surface plasmons in thin films," Phys. Rev. **182**(2), 539–554 (1969).
11. S. P. Morgan, Jr., "Effects of surface roughness on eddy current losses at microwave frequencies," J. Appl. Phys. **20**(4), 352–362 (1949).
12. M. V. Lukic, and D. S. Filipovic, "Modeling of 3-D surface roughness effects with application to coaxial lines," IEEE Trans. Microw. Theory Tech. **55**(3), 518–525 (2007).
13. R. Ding, L. Tsang, and H. Braunisch, "Wave Propagation in a Randomly Rough Parallel-Plate Waveguide," IEEE Trans. Microw. Theory Tech. **57**(5), 1216–1223 (2009).
14. H. Raether, *Surface Plasmons on Smooth and Rough Surfaces and on Gratings*, (Springer, Berlin, 1988).
15. J. A. Sánchez-Gil, "Localized surface-plasmon polaritons in disordered nanostructured metal surfaces: Shape versus Anderson-localized resonances," Phys. Rev. B **68**(11), 113410 (2003).
16. A. V. Zayats, I. I. Smolyaninov, and A. A. Maradudin, "Nano-optics of surface plasmon polaritons," Phys. Rep. **408**(3–4), 131–314 (2005).

#132570 - $15.00 USD Received 30 Jul 2010; revised 9 Sep 2010; accepted 9 Sep 2010; published 12 Oct 2010

17. A. Kolomenski, A. Kolomenskii, J. Noel, S. Peng, and H. Schuessler, "Propagation length of surface plasmons in a metal film with roughness," Appl. Opt. **48**(30), 5683–5691 (2009).
18. V. D. Freilikher, and S. A. Gredeskul, "Localization of waves in media with one-dimensional disorder," in *Progress in Optics*, E. Wolf, ed. (North-Holland, Amsterdam, 1996), V. XXX, pp. 137–203.
19. A. Lagendijk, B. van Tiggelen, and D. S. Wiersma, "Fifty years of Anderson localization," Phys. Today **62**(8), 24–29 (2009).
20. F. M. Izrailev, and N. M. Makarov, "Onset of delocalization in quasi-one-dimensional waveguides with correlated surface disorder," Phys. Rev. B **67**(11), 113402 (2003).
21. P. Lugan, A. Aspect, L. Sanchez-Palencia, D. Delande, B. Grémaud, C. A. Müller, and C. Miniatura, "One-dimensional Anderson localization in certain correlated random potentials," Phys. Rev. A **80**(2), 023605 (2009).
22. C. W. J. Beenakker, "Random-matrix theory of quantum transport," Rev. Mod. Phys. **69**(3), 731–808 (1997).
23. A. García-Martín, J. A. Torres, J. J. Sáenz, and M. Nieto-Vesperinas, "Transition from diffusive to localized regimes in surface corrugated optical waveguides," Appl. Phys. Lett. **71**(14), 1912–1914 (1997).
24. A. García-Martín, J. A. Torres, J. J. Sáenz, and M. Nieto-Vesperinas, "Intensity Distribution of Modes in Surface Corrugated Waveguides," Phys. Rev. Lett. **80**(19), 4165–4168 (1998).
25. J. A. Sánchez-Gil, V. Freilikher, I. Yurkevich, and A. A. Maradudin, "Coexistence of Ballistic Transport, Diffusion, and Localization in Surface Disordered Waveguides," Phys. Rev. Lett. **80**(5), 948–951 (1998).
26. F. D. Hastings, J. B. Schneider, and S. L. Broschat, "A Monte-Carlo FDTD Technique for Rough Surface Scattering," IEEE Trans. Antenn. Propag. **43**(11), 1183–1191 (1995).
27. E. I. Thorsos, "The validity of the Kirchhoff approximation for rough surface scattering using a Gaussian roughness spectrum," J. Acoust. Soc. Am. **83**(1), 78–92 (1988).
28. G. Veronis, and S. Fan, "Overview of Simulation Techniques for Plasmonic Devices," in *Surface Plasmon Nanophotonics*, Mark L. Brongersma and Pieter G. Kik, ed. (Springer, 2007).
29. E. D. Palik, *Handbook of Optical Constants of Solids*, (Academic, New York, 1985).
30. J. Jin, *The Finite Element Method in Electromagnetics*, (Wiley, New York, 2002).
31. S. Mazoyer, J. P. Hugonin, and P. Lalanne, "Disorder-induced multiple scattering in photonic-crystal waveguides," Phys. Rev. Lett. **103**(6), 063903 (2009).
32. J. D. Jackson, *Classical Electrodynamics* (Wiley, New York, 1999).
33. S. A. Maier, and H. A. Atwater, "Plasmonics: localization and guiding of electromagnetic energy in metal/dielectric structures," J. Appl. Phys. **98**(1), 011101 (2005).
34. C. F. Bohren, and D. R. Huffman, *Absorption and scattering of light by small particles*, (John Wiley & Sons, Inc., New York, 1983).
35. S. Hughes, L. Ramunno, J. F. Young, and J. E. Sipe, "Extrinsic optical scattering loss in photonic crystal waveguides: role of fabrication disorder and photon group velocity," Phys. Rev. Lett. **94**(3), 033903 (2005).
36. G. Veronis, and S. Fan, "Modes of subwavelength plasmonic slot waveguides," J. Lightwave Technol. **25**(9), 2511–2521 (2007).
37. T. Barwicz, and H. A. Haus, "Three-Dimensional Analysis of Scattering Losses Due to Sidewall Roughness in Microphotonic Waveguides," J. Lightwave Technol. **23**(9), 2719–2732 (2005).
38. C. G. Poulton, C. Koos, M. Fujii, A. Pfrang, T. Schimmel, J. Leuthold, and W. Freude, "Radiation Modes and Roughness Loss in High Index-Contrast Waveguides," IEEE J. Sel. Top. Quant. **12**(6), 1306–1321 (2006).
39. C. L. Holloway, and E. F. Kuester, "Power Loss Associated with Conducting and Superconducting Rough Interfaces," IEEE Trans. Microw. Theory Tech. **48**(10), 1601–1610 (2000).

1. Introduction

Plasmonic devices, based on surface plasmons propagating at metal-dielectric interfaces, have shown the potential to guide and manipulate light at deep subwavelength scales [1–5]. The propagation of surface plasmons can be strongly affected by fabrication-related disorders at metal-dielectric interfaces. Thus, for practical implementations of plasmonic devices, it is of fundamental importance to determine the sensitivity of the device properties to fabrication-related disorders.

In this paper, we theoretically investigate the effect of fabrication-related disorders on subwavelength metal-dielectric-metal (MDM) plasmonic waveguides. MDM plasmonic waveguides [6–8], which are the optical analogue of microwave two-conductor transmission lines [9], are of particular interest because they support modes with deep subwavelength scale and high group velocity over a very wide range of frequencies extending from DC to visible [10]. Thus, MDM waveguides could be potentially important in providing an interface between conventional optics and subwavelength electronic and optoelectronic devices.

Here we consider MDM waveguides in which both metal-dielectric interfaces are rough. In the case of a smooth MDM waveguide, there is optical power loss associated with the material loss in the metal, and characterized by an attenuation coefficient α_s. In a rough MDM waveguide, disorders induce additional attenuation on top of the material loss in the metal. The total optical power loss in the rough waveguide is characterized by an attenuation

#132570 - $15.00 USD Received 30 Jul 2010; revised 9 Sep 2010; accepted 9 Sep 2010; published 12 Oct 2010

coefficient α_r. Thus, the difference of attenuation coefficients α_r-α_s is a measure of the excess losses in the plasmonic waveguides due to disorders, and will be referred to as the excess attenuation coefficient due to disorder. We use the Monte Carlo method to calculate the attenuation coefficient α_r in a rough waveguide by averaging over an ensemble of randomly-generated rough waveguide realizations. For each randomly-generated rough waveguide realization, the electromagnetic fields are calculated using a full-wave finite-difference frequency-domain (FDFD) method. For small roughness root-mean-square (rms) height, the excess optical power loss due to disorder is small compared to the material loss in a smooth waveguide. However, for large roughness height, the excess attenuation increases rapidly with height, and the propagation length of the optical mode is severely affected. We find that the disorder loss is mainly due to reflection from the rough surfaces. However, for small roughness correlation lengths, enhanced absorption in the metal is the dominant loss mechanism due to disorder. We also find that the disorder attenuation due to reflection is approximately maximized when the power spectral density of the disordered surfaces at the Bragg spatial frequency is maximized. Finally, we show that increasing the modal confinement or decreasing the guide wavelength, increase the attenuation due to disorder in the MDM waveguide.

In previous studies, the effect of rough metal surfaces on electromagnetic wave propagation in the microwave frequency range has been investigated [11–13]. The effect of metal roughness on surface plasmons propagating at a single metal-dielectric interface at optical frequencies has also been investigated [14–17]. In addition, we note that the physics of light propagation in disordered MDM plasmonic waveguides is similar to that of wave transport and Anderson localization in one-dimensional disordered systems [18–20]. More specifically, the disorder loss due to reflection in MDM plasmonic waveguides is connected to Anderson localization in one-dimensional disordered systems. In such one-dimensional systems all states are localized for any disorder strength, and the localization length is proportional to the transport mean-free path [19,21,22]. In this context, several studies have investigated the localization of electromagnetic waves in disordered waveguides with perfectly conducting walls [20,23–25].

The remainder of the paper is organized as follows. In Section 2, we describe the simulation method used for the random rough surface generation and the analysis of the rough MDM waveguides. The results obtained using this method for the rough MDM waveguides are presented in Section 3. Finally, our conclusions are summarized in Section 4.

2. Simulation method

In Fig. 1(a), we show a schematic of the simulation configuration that we use to calculate the attenuation coefficient α_r of a rough MDM waveguide. It consists of a section of the rough waveguide of length L sandwiched between two smooth MDM waveguides. The roughness height function $f(x)$ at each metal-dielectric interface is assumed to be a one-dimensional statistical homogeneous random process with zero mean. The nature of the roughness is described by the autocorrelation function of $f(x)$ [13]

$$R(u) = < f(x) f(x+u) >,$$

where the brackets represent the ensemble average. We assume that both metal-dielectric interfaces are rough and mutually uncorrelated. We consider a realistic disorder model, in which the roughness height function $f(x)$ obeys Gaussian statistics and has a Gaussian autocorrelation function

$$R(u) = \delta^2 \exp(-u^2 / L_c^2), \tag{1}$$

where δ is the roughness rms height, and L_c is the correlation length [26]. We use a spectral method proposed by Thorsos [26,27] to randomly generate rough interface realizations. In this method, each rough interface consists of M discrete points spaced Δx apart over the surface length $L = M\Delta x$. Realizations are generated at $x_n = n\Delta x$ ($n = 1,\ldots, M$) using

#132570 - $15.00 USD Received 30 Jul 2010; revised 9 Sep 2010; accepted 9 Sep 2010; published 12 Oct 2010

$$f(x_n) = \frac{1}{L}\sum_{j=-M/2}^{M/2-1} F(k_j) e^{ik_j x_n}, \tag{2}$$

where, for $j \geq 0$,

$$F(k_j) = \sqrt{2\pi L W(k_j)} \cdot \begin{cases} [M(0,1) + iM(0,1)]/\sqrt{2}, & \text{for } j \neq 0, M/2 \\ M(0,1), & \text{for } j = 0, M/2 \end{cases}, \tag{3}$$

and for $j<0$, $F(k_j) = F(k_{-j})^*$. In Eqs. (2) and (3), $k_j = 2\pi j/L$, $M(0,1)$ is a number sampled from a Gaussian distribution with zero mean and unity variance, and $W(k)$ is the power spectral density of the rough surface. For a rough surface with Gaussian autocorrelation function (Eq. (1)), the power spectral density is [13,26,27]

$$W(k) \equiv \frac{1}{2\pi}\int_{-\infty}^{\infty} R(u) e^{-iku} du = \frac{\delta^2 L_c}{2\sqrt{\pi}} \exp(-\frac{k^2 L_c{}^2}{4}). \tag{4}$$

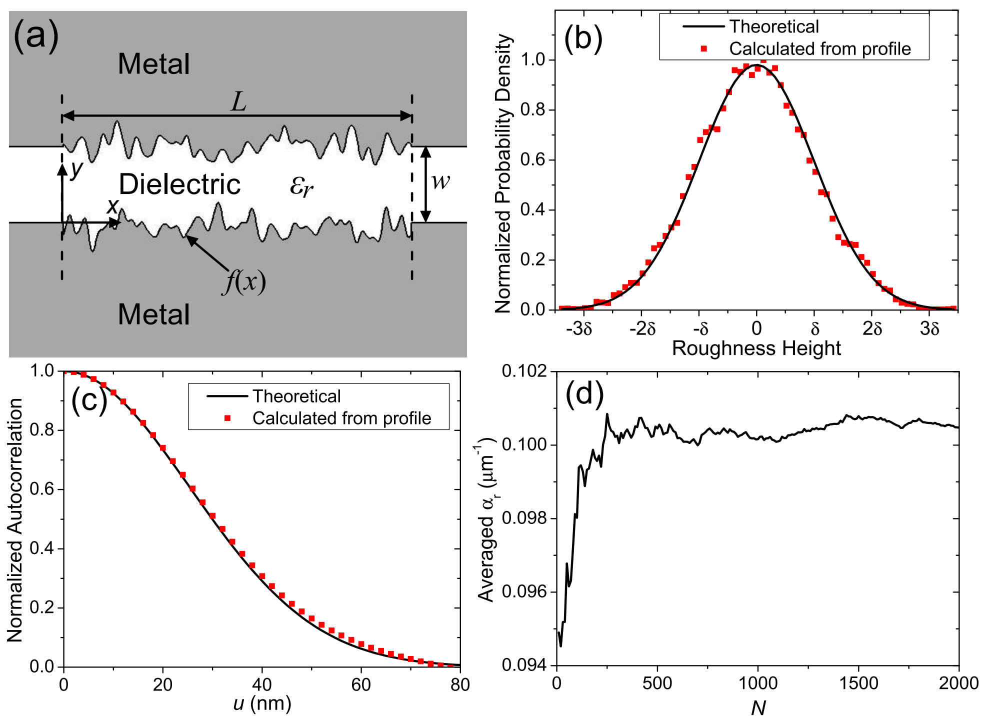

Fig. 1. (a) Schematic of the simulation configuration used to calculate the attenuation coefficient α_r of a rough MDM waveguide. It consists of a section of the rough waveguide of length L sandwiched between two smooth MDM waveguides. (b) Theoretical normalized probability density of the roughness height at metal-dielectric interfaces. We also show the probability density calculated from the generated profile of a random interface realization. (c) Theoretical normalized autocorrelation function $R(u) = \langle f(x)f(x+u)\rangle$ of the roughness. Results are shown for L_c = 36nm. We also show the autocorrelation function calculated from the generated profile of a random interface realization. (d) Averaged attenuation coefficient α_r as a function of the number N of random rough waveguide realizations used in the Monte Carlo method. Results are shown for a silver-air-silver MDM waveguide with w = 50nm, L = 2μm, L_c = 36nm, δ = 4nm, and λ = 1.55μm.

In Figs. 1(b) and 1(c), we show the probability density and autocorrelation function, respectively, for such a random interface realization calculated directly from one generated profile by the spectral method. We observe that they are both in excellent agreement with their

#132570 - $15.00 USD Received 30 Jul 2010; revised 9 Sep 2010; accepted 9 Sep 2010; published 12 Oct 2010

respective theoretical values, confirming the validity of the method that we use for random rough surface generation.

For each randomly-generated rough waveguide realization, we use a full-wave two-dimensional FDFD method [28] to calculate the electromagnetic fields and the transmission coefficient T through the waveguide section of length L (Fig. 1(a)). This method allows us to directly use experimental data for the frequency-dependent dielectric constant of materials such as silver [29], including both the real and imaginary parts, with no approximation. Perfectly matched layer absorbing boundary conditions [30] are used at all boundaries of the simulation domain. We also note that, since we directly use a full-wave simulation method to calculate the fields in the disordered waveguides, our calculations take into account multiple scattering and localization effects [31].

We use a Monte Carlo method [26] to average over an ensemble of randomly-generated rough waveguide realizations. We found that, as expected [22,31], $\langle\ln(T)\rangle$ undergoes a linear variation with L for large L. This allows us to define an attenuation coefficient α_r for the rough MDM waveguide using [31]

$$<\ln(T)>=-\alpha_r L. \qquad (5)$$

We note that α_r is referred to in the literature on disordered systems as the Lyapunov exponent and its inverse as the localization length [18,20–22]. In all cases we choose L large enough to ensure that Eq. (5) holds. In Fig. 1(d), we show a typical result for the convergence of the calculated attenuation coefficient α_r of a rough MDM plasmonic waveguide, as a function of the number N of randomly-generated rough waveguide realizations used in the Monte Carlo method. We observe that the method converges after a few hundred waveguide realization calculations. In all cases we found that N = 1000 is sufficient for an accuracy of the results within 1%.

3. Results

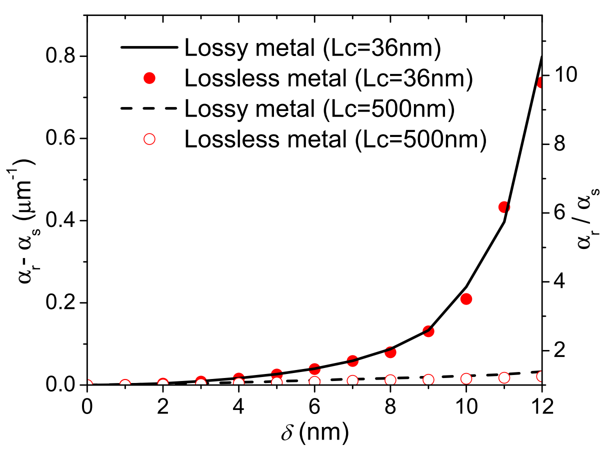

Fig. 2. Excess attenuation coefficient α_r-α_s of a rough MDM plasmonic waveguide and attenuation enhancement factor α_r/α_s with respect to a smooth waveguide as a function of roughness rms height δ for L_c = 36nm (solid line) and L_c = 500nm (dashed line). Also shown is the excess attenuation coefficient α_r-α_s of a rough MDM plasmonic waveguide as a function of δ for L_c = 36nm (filled circles) and L_c = 500nm (empty circles), if the metal in the MDM waveguide is lossless. All other parameters are as in Fig. 1(d).

We first consider the effect of the roughness rms height δ and correlation length L_c on the attenuation coefficient. In Fig. 2, we show the excess attenuation coefficient α_r-α_s of a rough MDM plasmonic waveguide as a function of the roughness rms height δ for L_c = 36nm. For convenience we also show the attenuation enhancement factor, defined as α_r/α_s. We observe that, as expected, the excess attenuation coefficient α_r-α_s increases with δ. We also found that for δ>4nm, the increase is almost exponential. For δ<4nm, we have α_r/α_s<1.2 for the

#132570 - $15.00 USD Received 30 Jul 2010; revised 9 Sep 2010; accepted 9 Sep 2010; published 12 Oct 2010

attenuation enhancement factor. Thus, for small roughness height (δ<4nm), the excess optical power loss due to disorder is small compared to the material loss in a smooth waveguide. On the other hand, for large roughness height (δ>4nm), α_r/α_s increases rapidly with δ, and the propagation length of the optical mode is severely affected. Thus, for δ = 12nm the attenuation coefficient in the rough waveguide is enhanced by an order of magnitude compared to the smooth waveguide ($\alpha_r/\alpha_s \approx 10$).

In Fig. 2, we also show the excess attenuation coefficient α_r-α_s for a rough MDM waveguide in which the metal in the MDM waveguide is lossless ($\varepsilon_{\text{metal}} = \varepsilon_{\text{metal,real}}$, neglecting the imaginary part of the dielectric permittivity $\varepsilon_{\text{metal,imag}}$). We observe that material losses in the metal do not significantly affect the excess attenuation coefficient α_r-α_s. In the lossless metal case, α_s = 0 and the excess attenuation is only due to the reflection from the rough surfaces. Thus, we can conclude that the excess loss in a rough MDM plasmonic waveguide is mainly due to reflection from the rough surfaces. As mentioned in Section 1, this loss mechanism is connected to Anderson localization in one-dimensional disordered systems.

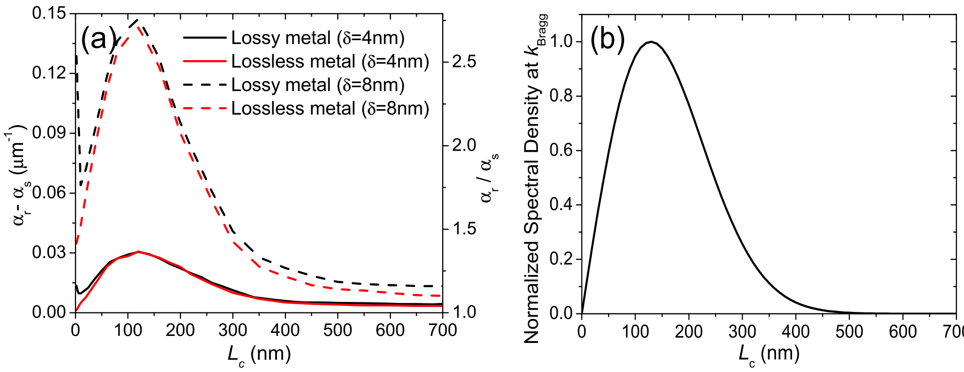

Fig. 3. (a) Excess attenuation coefficient α_r-α_s of a rough MDM plasmonic waveguide and attenuation enhancement factor α_r/α_s as a function of correlation length L_c for δ = 4nm (black solid line) and δ = 8nm (black dashed line). Also shown is the excess attenuation coefficient α_r-α_s of a rough MDM plasmonic waveguide as a function of L_c for δ = 4nm (red solid line) and δ = 8nm (red dashed line), if the metal in the MDM waveguide is lossless. All other parameters are as in Fig. 1(d). (b) Normalized power spectral density of the disordered surfaces at the Bragg spatial frequency k_{Bragg} as a function of L_c. All other parameters are as in Fig. 1(d).

In Fig. 3(a), we show the excess attenuation coefficient α_r-α_s and the attenuation enhancement factor α_r/α_s of a rough MDM plasmonic waveguide as a function of the correlation length L_c for δ = 4nm, 8nm. We observe that in both cases α_r-α_s is maximized for L_c = 120nm. In addition, the excess attenuation coefficient α_r-α_s increases as $L_c \to 0$. In Fig. 3(a), we also show the excess attenuation coefficient α_r-α_s for a rough MDM waveguide in which the metal in the MDM waveguide is lossless. The results in the lossless metal case agree well with the lossy metal case for L_c>20nm. Thus, we can conclude that for L_c>20nm, the excess attenuation is due to reflection from the rough surfaces.

We found that the peak in excess attenuation coefficient α_r-α_s at L_c = 120nm is associated with Bragg reflection from the rough surfaces. In a MDM plasmonic waveguide with a periodic perturbation with period P, there is strong reflection associated with Bragg Scattering [4] when

$$P = P_{Bragg} = \lambda_{MDM} / 2,$$

where λ_{MDM} is the guide wavelength in the MDM plasmonic waveguide. The corresponding Bragg spatial frequency is

$$k_{Bragg} \equiv \frac{2\pi}{P_{Bragg}} = \frac{4\pi}{\lambda_{MDM}}. \tag{6}$$

#132570 - $15.00 USD Received 30 Jul 2010; revised 9 Sep 2010; accepted 9 Sep 2010; published 12 Oct 2010

Using Eqs. (4) and (6), we obtain the power spectral density $W(k_{Bragg})$ of the disordered surfaces at k_{Bragg}

$$W(k_{Bragg}) = \frac{\delta^2 L_c}{2\sqrt{\pi}} \exp[-(\frac{2\pi L_c}{\lambda_{MDM}})^2]. \tag{7}$$

In Fig. 3(b), we show $W(k_{Bragg})$ as a function of L_c. We observe that the excess attenuation coefficient α_r-α_s due to reflection from disorders correlates very well with the power spectral density $W(k_{Bragg})$. Thus, the disorder attenuation due to reflection is approximately maximized when the power spectral density of the disordered surfaces at the Bragg spatial frequency $W(k_{Bragg})$ is maximized. Using Eq. (7), we find that $W(k_{Bragg})$ is maximized for $L_c = \frac{\lambda_{MDM}}{2\sqrt{2}\pi}$.

For L_c<20nm, there is a large difference between the lossy and lossless metal cases (Fig. 3(a)). In the lossless metal case, the excess attenuation coefficient α_r-α_s decreases as $L_c \to 0$, due to the fact that $\lim_{L_c \to 0} W(k_{Bragg}) = 0$. However, in the lossy metal case the excess attenuation coefficient α_r-α_s increases as $L_c \to 0$. This is because when $L_c \to 0$, the waveguide surfaces become extremely rough with disorder dimensions small compared to the skin depth, which allows light to directly pass through, and results in enhanced absorption in the metal. Thus, for L_c<20nm, the reflection from the rough surfaces is small, and enhanced absorption in the metal is the dominant loss mechanism due to disorder. Finally, for very large correlation lengths (L_c>400nm), the waveguide surfaces are almost flat, which results in a small reflection, hence the attenuation coefficient is only slightly enhanced with respect to the smooth waveguide (Figs. 2, 3(a)).

We further investigate the enhanced absorption in disordered MDM plasmonic waveguides by considering the electromagnetic field distribution in such waveguides. In Fig. 4(a) we show the electric field intensity profile for a random rough MDM plasmonic waveguide. Since metals satisfy the condition $|\varepsilon_{metal}| >> \varepsilon_{diel}$ at near-infrared wavelengths [29], the electric field intensity in the metal is much smaller than the electric field intensity in the dielectric. In addition, we observe that the electric field intensity in the dielectric is enhanced at the peak of the metal roughness bumps. The enhancement is associated with the behavior of the electric field near sharp edges [32], which is often referred to as the lightning rod effect [33]. The increased surface charge density at the metal bump peak leads to crowding of the electric field lines in the dielectric, and therefore to enhancement of the near field in the vicinity of the bump peak.

The absorbed power density depends, however, on the electric field intensity in the metal. In Fig. 4(c) we show the absorbed power density profile in the metal for the random rough MDM waveguide. Contrary to the electric field intensity in the dielectric, the electric field intensity in the metal, and therefore the absorbed power density, is maximum (minimum) at the bottom (peak) of the metal roughness bumps. Thus, in a rough MDM waveguide absorption is enhanced with respect to a smooth waveguide at the bottom of metal roughness bumps. In Fig. 4(e) we also show the local absorption coefficient $\alpha_r(x)$ for the random rough MDM waveguide. We observe that in certain locations of the disordered waveguide, corresponding to peaks of metal roughness bumps, the absorption is actually suppressed with respect to a smooth MDM waveguide. Even though the absorption is locally suppressed at certain locations, the overall absorption in the rough waveguide is enhanced with respect to the smooth waveguide. As mentioned above, this absorption enhancement is the dominant disorder loss mechanism in the case of small roughness correlation length. We finally note that the absorption properties described above are quite general and are not limited to random rough waveguides. As an example, periodically textured waveguides exhibit similar characteristics (Figs. 4(b), 4(d), 4(f)).

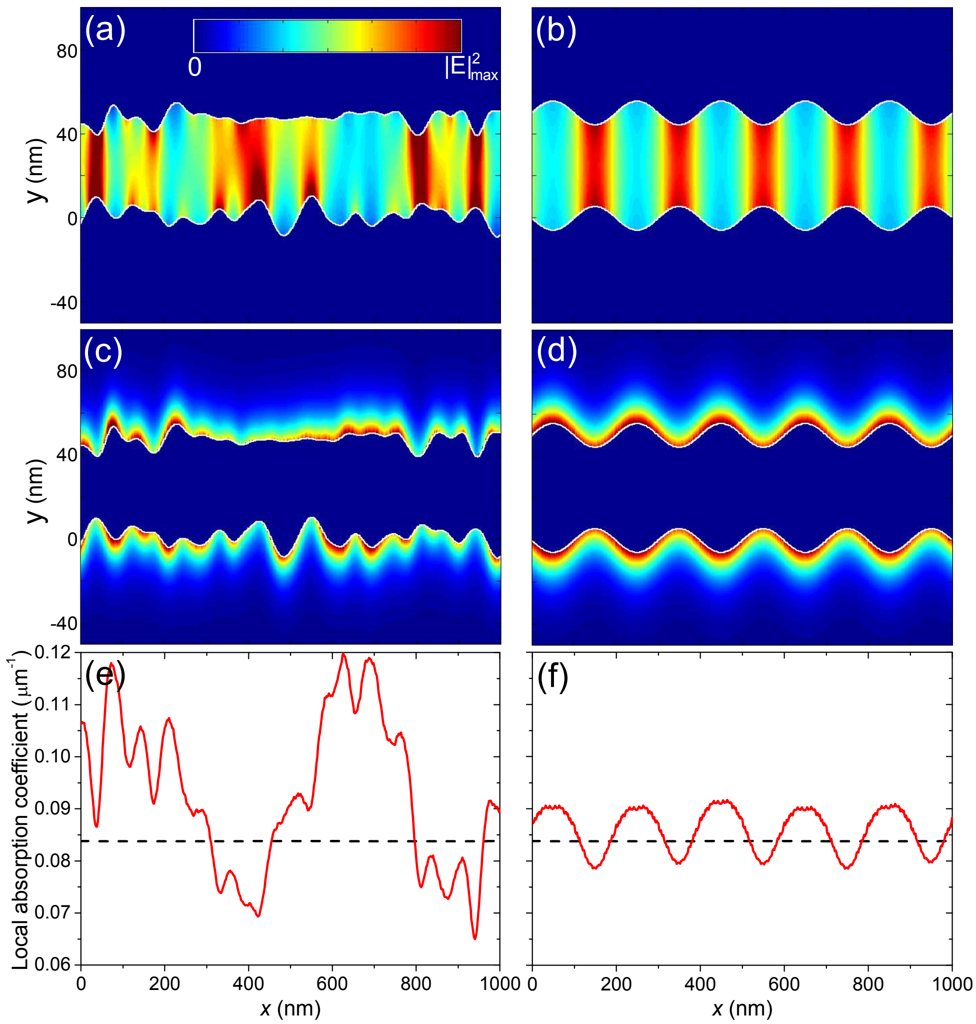

Fig. 4. (a)-(b) Electric field intensity profiles for a random rough MDM plasmonic waveguide and a MDM waveguide with periodic perturbation. Results are shown for perturbation periodicity P = 200nm and amplitude $A = 2\sqrt{2}\delta$ in the sine periodic waveguide. All other parameters are as in Fig. 1(d). (c)-(d) Absorbed power density profiles for a random rough MDM waveguide and a MDM waveguide with periodic perturbation. (e)-(f) Local absorption coefficient for a random rough MDM plasmonic waveguide and a MDM waveguide with periodic perturbation. We also show the local absorption coefficient for a smooth MDM waveguide (black dashed line).

We finally consider the effect of the MDM waveguide parameters, such as waveguide width w, operating wavelength λ, and dielectric constant ε_r of the material in the waveguide (Fig. 1(a)), on the attenuation in the rough MDM plasmonic waveguides. In Figs. 5(a) and 5(d), we show the attenuation coefficient α_s in a smooth MDM waveguide, and the excess attenuation coefficient due to disorder α_r-α_s, respectively, as a function of the waveguide width w. In a smooth MDM waveguide, the fraction of the modal power in the metal increases as w decreases, and the attenuation coefficient α_s therefore increases (Fig. 5(a)) [6].

We also observe that, as w decreases and the optical mode confinement increases, the effect of the roughness becomes more severe (Fig. 5(d)). Several factors contribute to the increased disorder losses when w is decreased. First, as w decreases, the ratio δ/w of roughness rms height to waveguide width increases, and the fraction of the modal power reflected by disorders, therefore, increases. Second, as w decreases, the fraction of the modal

#132570 - $15.00 USD Received 30 Jul 2010; revised 9 Sep 2010; accepted 9 Sep 2010; published 12 Oct 2010

power in the metal increases, and the effective index of the propagating mode, therefore, increases. Thus, the guide wavelength λ_{MDM} decreases. This in turn leads to increased disorder losses, since the scattering cross-section of metallic nanoparticles increases as the wavelength decreases [4,34]. Third, as w decreases, the group velocity of the propagating optical mode in the MDM plasmonic waveguide decreases. This in turn leads to increased disorder losses, since a smaller group velocity means that light moves more slowly through the waveguide and thus has more time to sample the regions of disorder and roughness [31,35]. In short, increasing the light confinement in a MDM plasmonic waveguide leads to increased ratio of disorder size to waveguide width, decreased guide wavelength, and decreased group velocity, and, therefore, to increased disorder losses.

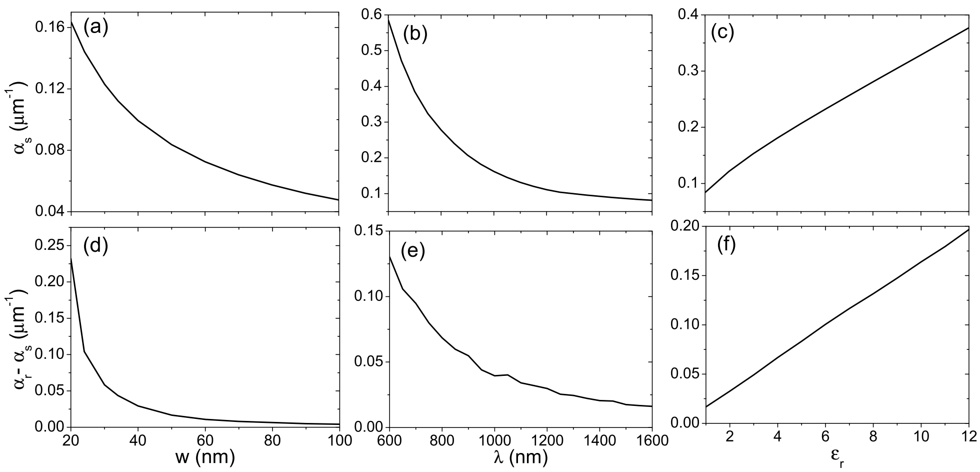

Fig. 5. (a)-(c) Attenuation coefficient α_s in a smooth MDM plasmonic waveguide as a function of width w, wavelength λ, and dielectric constant ε_r of the material in the waveguide. All other parameters are as in Fig. 1(d). (d)-(f) Excess attenuation coefficient due to disorder α_r-α_s as a function of w, λ, and ε_r. All other parameters are as in Fig. 1(d).

In Figs. 5(b) and 5(e), we show the effect of operating wavelength λ on the attenuation coefficient in a smooth waveguide α_s, and the excess attenuation coefficient due to disorder α_r-α_s, respectively. In a smooth MDM waveguide the attenuation coefficient α_s increases as the wavelength decreases (Fig. 5(b)). This is due to the fact that the propagation length of surface plasmons scales with the wavelength [1], since the fraction of the modal power in the metal increases at shorter wavelengths, and also due to increased material losses of metals at shorter wavelengths [29]. In addition, we observe that the excess attenuation due to roughness increases as the wavelength decreases (Fig. 5(e)). This is due to the fact that, as the operating wavelength decreases, the guide wavelength and the group velocity decrease. Both of these factors contribute to increased disorder losses, as mentioned above.

In Figs. 5(c) and 5(f), we show the effect of dielectric constant ε_r of the material in the waveguide (Fig. 1(a)) on the attenuation coefficient in a smooth waveguide α_s, and the excess attenuation coefficient due to disorder α_r-α_s, respectively. In a smooth MDM waveguide α_s increases with ε_r (Fig. 5(c)). This is due in part to increased fraction of the modal power in the metal, as the permittivity of the dielectric increases, as well as decreased group velocity. In addition, we observe that the excess attenuation due to roughness also increases with ε_r (Fig. 5(f)). This is due to the fact that, as the permittivity of the dielectric increases, the guide wavelength and the group velocity decrease. Both of these factors contribute to increased disorder losses, as mentioned above.

4. Conclusions

In this paper we investigated the effect of fabrication-related disorders on the properties of subwavelength MDM plasmonic waveguides. We used a realistic model for the random rough

#132570 - $15.00 USD Received 30 Jul 2010; revised 9 Sep 2010; accepted 9 Sep 2010; published 12 Oct 2010

surfaces in which the roughness height function $f(x)$ obeys Gaussian statistics and has a Gaussian autocorrelation function. We used the FDFD method to simulate each randomly-generated rough waveguide realization, and the Monte Carlo method to average over an ensemble of random realizations.

We considered the effect of the roughness rms height δ and the correlation length L_c on the excess attenuation coefficient α_r-α_s. For small roughness rms height, the reflection from the rough surfaces is small, hence the excess optical power loss due to disorder is small compared to the material loss in a smooth waveguide. For large roughness height, α_r/α_s increases rapidly with δ, and the propagation length of the optical mode is severely affected. We found that excess loss in rough MDM plasmonic waveguides is mainly due to reflection from the rough surfaces. However, for small roughness correlation lengths, enhanced absorption in the metal is the dominant loss mechanism due to disorder. We also found that the disorder attenuation due to reflection is approximately maximized when the power spectral density of the disordered surfaces at the Bragg spatial frequency is maximized.

We also considered the electromagnetic field distribution in disordered MDM plasmonic waveguides to further investigate the enhanced absorption in such waveguides. We found that the electric field intensity in the metal, as well as the absorbed power density, is maximum (minimum) at the bottom (peak) of the metal roughness bumps. The local absorption coefficient for the disordered waveguide can be enhanced or suppressed with respect to a smooth MDM waveguide at different locations. Even though the absorption is locally suppressed at certain locations, the overall absorption in the rough waveguide is enhanced with respect to the smooth waveguide.

Finally, we considered the effect of the MDM waveguide parameters, such as waveguide width w, operating wavelength λ, and dielectric constant ε_r of the material in the waveguide, on the attenuation in rough MDM plasmonic waveguides. We found that variation of these waveguide parameters impacts several important factors that affect disorder losses, such as the ratio of disorder size to waveguide width, the guide wavelength, and the group velocity. Increasing the light confinement in a MDM plasmonic waveguide leads to increased ratio of disorder size to waveguide width, decreased guide wavelength, and decreased group velocity, and, therefore, to increased disorder losses.

As final remarks, we note that the two-dimensional model that we used here should also accurately describe the case of three-dimensional subwavelength plasmonic slot waveguides [36] with large height to width aspect ratio. In three-dimensional nanophotonic waveguides the sidewall roughness, which arises due to imperfections in the etching process, most often appears as long vertical stripes. The roughness can therefore be represented by a one-dimensional random process, similar to the one we used here [37,38]. In addition, in the three-dimensional case, out-of-plane radiation loss is an additional disorder loss mechanism. However, based on previous studies on three-dimensional microwave metallic waveguides [39], and photonic crystal waveguides [31], we expect this disorder loss mechanism to be less significant for three-dimensional plasmonic slot waveguides than reflection and enhanced absorption.

Acknowledgments

This research was supported by the Louisiana Board of Regents (Contract No. LEQSF(2009-12)-RD-A-08).